HTD-Vol. 176, Heat and Mass Transfer in
Fires and Combustion Systems
ASME 1991

TIME-DEPENDENT LOCAL MASS LOSS RATE OF FINITE-THICKNESS BURNING WALLS OF PMMA

A. K. Kulkarni and C. I. Kim
Department of Mechanical Engineering
Pennsylvania State University
University Park, Pennsylvania

H. E. Mitler
Building and Fire Research Laboratory
National Institute of Standards and Technology
Gaithersburg, Maryland

Abstract

This paper discusses transient local mass loss rate, $\dot{m}''(t)$, behavior of burning vertical walls of finite thickness. Comparison of data and predictions are made for polymethylmethacrylate (PMMA) slabs, although both experimental and analytical model presented here can be easily extended to study other wall materials. The experimental setup is designed to simulate wall pyrolysis in a typical wall fire situation. Samples of wall materials are burnt under the presence of turbulent flames while their weight is continuously monitored; $\dot{m}''(t)$ is thereby determined. The analysis assumes that the pyrolysis occurs in depth (rather than only at the surface), described by a first order Arrhenius reaction. Unsteady heat loss into the interior of the finite-thickness wall is taken into consideration to arrive at the net, transient, local mass loss rate prediction. Prediction and the data obtained in the mass loss rate apparatus for a 3.2 mm thick PMMA slab compare well. The local mass loss rate function, $\dot{m}''(t)$, when properly measured and appropriately used in analytical models, may be treated as a material "fire property," and it is also presented for two other wall materials.

Nomenclature

$a_{0\text{-}4}$ = constants in Eq. (1)
c_p = specific heat of slab, J/kg-K
H_v = effective heat of vaporization
k = thermal conductivity, W/m-K
L = thickness of the slab, m
L_v = latent heat of vaporization, J/kg
$\dot{m}''$ = mass loss rate per unit area, kg/m^{2}s
$\dot{m}'''$ = mass loss rate per unit volume, kg/m^{3}s
t = time, s
$T(x,t)$ = temperature of the slab at depth x and time t, K
T_a = initial temperature, K
T_A = activation temperature, K
T_p = pyrolysis temperature, K
T_o = ambient temperature, K
T_s = surface temperature, K
α_w = absorptivity of the surface (taken to be a grey body)
δ = characteristic thermal depth, m
ϕ_c = convective heat flux to (from) surface, kW/m^2
ϕ_{ext} = external (radiative) flux impinging on the surface, kW/m^2
ϕ_{net} = net flux into the surface, kW/m^2
ϕ_{rf} = radiative heat flux from the wall flame, kW/m^2
ϕ_{rr} = reradiative heat flux from surface, kW/m^2
λ = time from onset of pyrolysis, s
λ_b = burnout time, s
ζ = inverse of a time constant defined in Eq. (12), s^{-1}

Introduction

The local mass loss (or burning) rate, $\dot{m}''$, of a vertical wall is an important variable in many fire-related problems, such as flame spread on a wall, fire growth and energy release rate in an enclosure fire, and the spread of smoke and hot gas plumes. For prediction of upward flame

spread on a vertical wall, flame height must be calculated, which depends on the total energy release rate; that, in turn, is directly influenced by the local mass loss rate integrated over the entire pyrolyzing area of the wall. At a given location the mass loss rate is usually a strongly transient function, which depends on such factors as the external and flame heat feedback, heat conduction to the interior of the wall, material characteristics, and wall thickness. In the case of wood, for example, the burning rate peaks in the early stage of combustion due to volatile gases escaping the surface, and then tapers off as the char continues to burn. For thick polymer materials, the mass loss rate may continue to rise for an extended period due to the decreasing heat conduction to the interior. The wall thickness determines the burnout time, the time required to completely exhaust the normally combustible fraction of the wall at a given location. Thus, the local mass loss rate rises from zero at the start, goes back to zero at the burnout time, and behaves in a manner dictated by the earlier-mentioned factors, in between. It is imperative, therefore, that the local mass loss rate function $\dot{m}''(t)$, which, as explained later may be termed a "fire property" of a wall material, be known reasonably accurately for further use in other problems. The objectives of the present work were to devise a simple small scale experiment to obtain the transient mass loss rate function $\dot{m}''(t)$ for practical wall materials, to develop an algorithm for predicting $\dot{m}''(t)$ for a class of wall materials, and to compare the algorithm predictions with the data from the experiment, using slabs of polymethylmethacrylate (PMMA) as the test material.

There have been several attempts at the modeling of burning rate of wall fires. Local mass loss rate for a steadily burning semi-infinite slab of fuel with laminar flames can be obtained using natural convection boundary layer theory with heat and mass transfer analogy, with a known constant heat of vaporization (Kosdon, 1969; Kim, 1971). For turbulent wall fires, empirical correction factors for heat and mass transfer have been employed using turbulent Prandtl number and modified Reynold's analogy (Ahmad, 1978). Orloff and others (1977) proposed a correlation for local burning rate of PMMA for turbulent fires on thermally thick walls. However, all these local mass loss rates were for steady state burning of vertical walls. Delichatsios and de Ris (1983) proposed an expression for unsteady burning of charring fuels based on the balance of heat fluxes at the surfaces and the way the fluxes are affected by the growing char layer. Delichatsios (1987) also presented a method involving a more detailed system of equations for prediction of local mass loss rate of turbulent wall fires.

Recently, Mitler (1988) derived an expression for $\dot{m}''(t)$ for steadily burning slabs of PMMA in a room fire situation where significant amount of external radiation heat fluxes were present with a vertical variation of room conditions due to stratification. Based on the integration of local burning rate over the entire height of the pyrolysis zone, he was able to predict the total burning rate of the burning PMMA wall as a function of time which agreed very well with experiments. It has been shown experimentally that free-burning, 2 cm-thick slabs of PMMA have a strongly time-dependent mass loss rate for the first 1000 s (Kim, 1990a). It is clear that the local burning rate is indeed an important variable in the burning of vertical slabs which must be properly accounted for in the prediction of many fire-related phenomena. The overall purpose of the present investigation is to capture the specific behavior of materials burning in a vertical, flat surface configuration, in the form of $\dot{m}''(t)$ as a "fire property" of the wall material in a systematic way, using experiments and analysis.

Experiments

The primary motivation for obtaining the transient local mass loss rate was to describe the behavior of a burning vertical wall in the upward flame spreading situation where the unburnt fuel just above the pyrolysis front is continuously draped over by the flames issued by the burning region under it. Therefore, it was desirable to obtain $\dot{m}''(t)$ for a material sample under similar conditions. It has been observed experimentally (Quintiere, 1986) that the unburnt fuel above the pyrolysis front is subjected to a heat flux in the remarkably narrow range of 20 to 30 kW/m^2 by flames due to the combustion of pyrolyzed fuel coming from the burning region under the pyrolysis front. This has been observed for burning vertical walls of many different solid materials for energy release rates of 20 kW/m to 80 kW/m or a fire scale of up to approximately two meters, which is the normal room height (Quintiere, 1988). Therefore the local, transient mass loss rate measured under the "flaming" condition, i.e. the rate measured while a small material sample is completely draped over by turbulent wall flames originating at a distance upstream, is taken to be the material "fire property," to be used in analysis and for comparison purposes for most room fires. Even though the $\dot{m}''(t)$ function may not be a completely

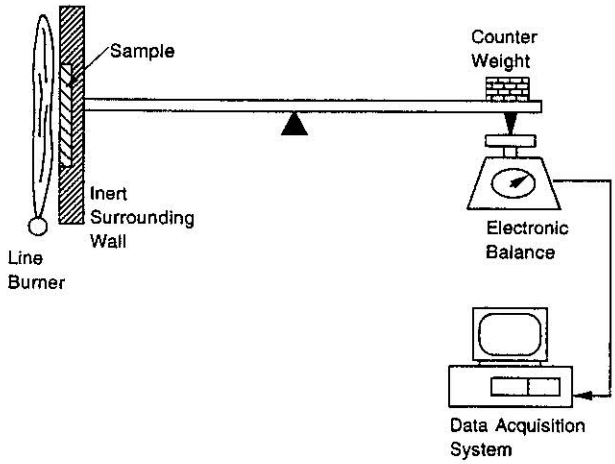

Figure 1. A Schematic of the Apparatus for Local Mass Loss Rate Measurements.

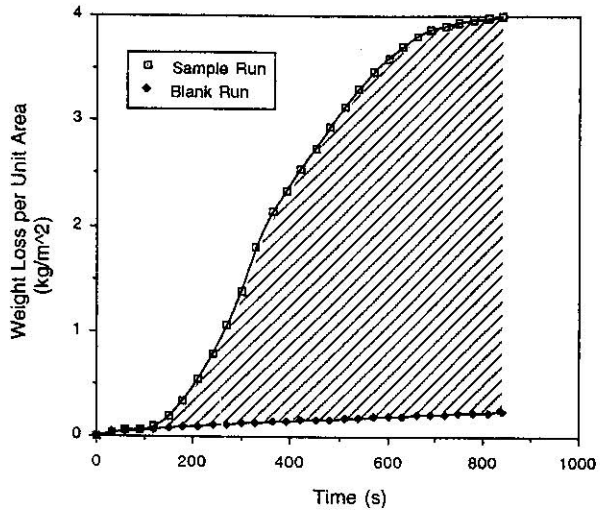

Figure 2. Measured mass loss rate for a 3.2 mm thick PMMA sample and with no sample (blank run) as a funciton of time. The hatched area indicates corrected mass loss rate.

accurate description of local mass rate, it is far better than assuming a constant burning rate. This property takes into account the specific character of the material and geometry and it is only weakly dependent on the vertical location for a fire scale of about 2 m. During the upward flame spread the unburnt material just ahead of the pyrolysis front will be subjected to conditions similar to those present in the measurement of $\dot{m}''(t)$. An important point is that $\dot{m}''(t)$ be measured for materials as they burn in the actual case; for example, if a wall is made of a 3.2 mm masonite panel mounted on a 12.7 mm marinite (inert) substrate, it be used in the same configuration to obtain $\dot{m}''(t)$. The $\dot{m}''(t)$ thus measured can be very effectively used in fire-related models, such as upward flame spread (Kim, 1990b).

The apparatus is shown in Figure 1. It includes an electronic balance with a digital display and analog output port, a structure made of aluminum beams, a mounting plate for the sample, a surrounding wall that covers the mounting plate, and a counterweight. A 12 cm × 12 cm sample is first mounted on a marinite plate (in order to simulate a wall panel mounted on a dry wall) and then held flush in a larger (24 cm × 30 cm) marinite plate attached to aluminum beams. The sample is ignited with a line burner using natural gas as fuel, with an energy release rate of 18 kW/m and an average flame tip height of 29 cm. The height of the burner flame is sufficient to cover the sample totally with turbulent flames because there is a clearance between the burner and the bottom of the sample. The total heat flux from burner flames to the sample location was found to be 27.5 ± 2.5 kW/m ^{2} in the absence of the sample.

The structure between the sample and the counterweight is maintained horizontal using a level gage. The mass loss of the sample results in a change of the weight that the balance displays. The analog output of the balance is connected to an automatic data acquisition system. The electronic balance has a range of 0-500 g and has an accuracy of ±0.02 g.

Since the inert plate surrounding the sample loses weight due to drying caused by heating, and a possible slight distortion of aluminum beams may affect the data, several blank runs were made with no sample mounted, and this systematic error is corrected every time before processing the data further. Figure 2 shows the actual mass loss data for a PMMA sample and the data without any sample (blank run). The final data for the time history of the mass of the sample, the difference between the two curves, are shown by shaded area in Figure 2. Because of the differentiation required on the data to obtain $\dot{m}''(t)$, the data had to be fitted with a smooth function. An examination of the data suggested a fourth or higher order polynomial; therefore, the mass loss rate data were fitted to a fifth order polynomial, which became a fourth order polynomial for $\dot{m}''(\lambda)$, given by,

$$\dot{m}''(\lambda) = \begin{cases} a_0 + a_1 \lambda + a_2 \lambda^2 + a_3 \lambda^3 + a_4 \lambda^4, & \text{if } \lambda < \lambda_b \\ 0, & \text{if } \lambda > \lambda_b \end{cases} \quad (1)$$

where λ is the time measured after the beginning of pyrolysis at a specific location, and λ_b is the burnout time, defined by

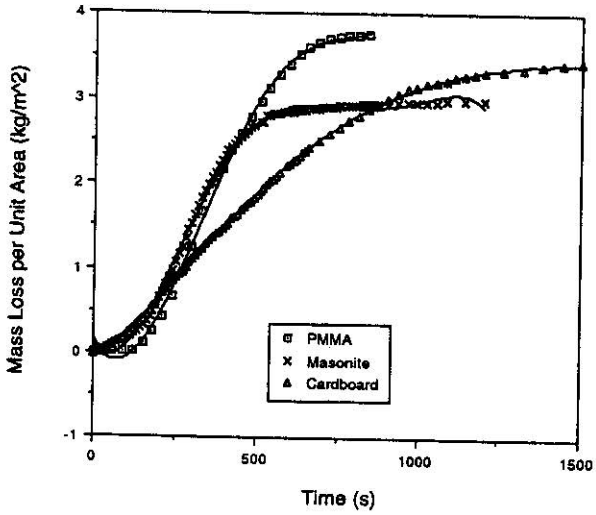

Figure 3. Measured mass loss per unit area (symbols) for three different materials and a polynomial curve fit (solid line) for each material.

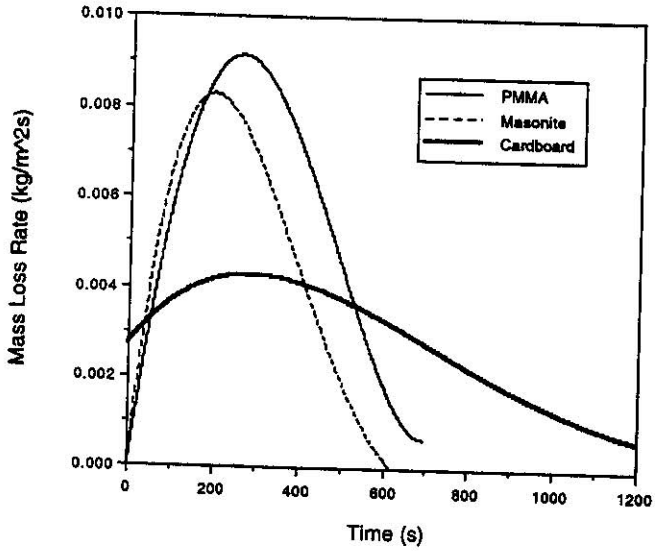

Figure 4. Mass loss rates as a function of time derived from curve-fits of Fig. 3.

$$\int_0^{\lambda_b} \dot{m}''(t)\, dt = m'' \qquad (2)$$

where m" is the combustible mass per unit area for a given sample.

The local mass loss rate was measured for three different materials: 3.2 mm-thick PMMA, 3.2 mm-thick masonite, and 5.0 mm-thick cardboard. Figure 3 shows the mass loss data as a function of time and the curve fits for the three materials. The mass loss rates derived from these data are given by the following expressions:

PMMA : $\dot{m}''(\lambda) = 1.723\times10^{-9} + 7.396\times10^{-5}\,\lambda - 1.551\times10^{-7}\,\lambda^2 - 6.566\times10^{-12}\,\lambda^3 + 1.130\times10^{-13}\,\lambda^4$, $\lambda_b = 693$ s,

Masonite : $\dot{m}''(\lambda) = 5.692\times10^{-10} + 1.011\times10^{-4}\lambda - 3.865\times10^{-7}\lambda^2 + 4.811\times10^{-10}\,\lambda^3 - 1.949\times10^{-13}\,\lambda^4$, $\lambda_b = 619$ s, and

Cardboard : $\dot{m}''(\lambda) = 2.727\times10^{-3} + 1.246\times10^{-5}\lambda - 3.028\times10^{-8}\lambda^2 + 2.143\times10^{-11}\,\lambda^3 - 5.048\times10^{-15}\,\lambda^4$, $\lambda_b = 1180$ s.

Figure 4 shows the mass loss rate functions for the three materials, obtained by the differentiation of the mass loss polynomial curve-fits.

Theory

The local, time-dependent mass loss rate of a wall material is modeled for noncharring fuels (like PMMA) of finite thickness, to arrive at an expression for $\dot{m}''(t)$. Here, the key mechanism assumed for estimating the pyrolysis rate is that the mass loss occurs in depth, not just at the surface, and that it can be expressed as an Arrhenius-type reaction with a known activation energy (or activation temperature). Other assumptions are mentioned as needed in the following derivation of the mass loss rate.

Assuming that heat transfer inside the material is by heat conduction only, the mass loss rate from the surface of a semi-infinite ablating slab is given by (Mitler, 1988)

$$\dot{m}'' = [\, \alpha_w \phi_{in} + \phi_c - \phi_{rr} + k\, \nabla T \,] / H_V \qquad (3)$$

where

$$H_V = L_V + \int_{T_a}^{T_p} c_p(T)\, dT \qquad (4)$$

is the effective heat of vaporization (or pyrolysis), L_V is the latent heat of vaporization, T_a is the initial temperature, T_p is the pyrolysis temperature, $-k\,\nabla T = \phi_{loss}$ is the heat flux diffusing into the solid, and the remaining terms are defined in the Nomenclature section.

Even if all the other terms on the right-hand side in Eq. (3) are constant, the temperature gradient decreases with time, as the thermal wave moves inward. Thus the loss term ($k\,\nabla T$) becomes smaller with time, and therefore $\dot{m}''$ increases with time. If the temperature gradient at x=0 approaches zero, $\dot{m}''$ will increase asymptotically to the steady-state value given by

$$\dot{m}'' = [\, \alpha_w \phi_{in} + \phi_c - \phi_{rr} \,] / H_V \equiv \phi_{net} / H_V \,. \qquad (5)$$

Physically, this can be understood as follows. The mass loss rate per unit area is

$$\dot{m}'' = \int \dot{m}'''(z)\, dz \tag{6}$$

where the limits are zero (the surface) and infinity for a semi-infinite slab. $\dot{m}'''(z)$ is the local volumetric mass depletion rate (in gm/m^{3}sec). It is a strongly increasing function of temperature. Since the temperature decreases from the surface, so does the production rate, and significant pyrolysis is seen to take place mainly near the surface. Equations (3) and (4) give the energy balance at the front surface of the material, whereas the mass loss, as discussed, in fact occurs in depth.

Thus, if we can find $k\nabla T$, we will — assuming T_p is constant — have found $\dot{m}''$ as a function of t. We approximate the temperature distribution in the slab by

$$T(x,t) - T_o \cong \theta_p\, e^{-x/\delta(t)} \tag{7}$$

where $$\theta_p \equiv T_p - T_o. \tag{7a}$$

From the reasoning above, $\delta(t)$ increases with time. If the mass loss rate approaches a constant value with a constant net flux, that corresponds to δ reaching a constant value. Eq. (7) implies that the heat diffusion into the slab at the surface is

$$\phi_{loss} = -k\,(\nabla T)_o \cong k\,(T(0,t) - T_o)\,/\,\delta(t) = k\,\theta_p\,/\,\delta(t) \tag{8}$$

It is readily found that

$$\delta_o \equiv \delta(0) = k\theta_p\,/\,\phi_{net}\,, \tag{9}$$

and that

$$\delta_\infty = \delta(\infty) = (H_V\,/\,c_p\theta_p)\,\delta_o\,. \tag{10}$$

Finally,

$$\delta(t) = \delta_\infty - (\delta_\infty - \delta_o)\,exp(-\zeta\, t) \tag{11}$$

where

$$\zeta = 2\,\phi_{net}\,/\,[\,\rho\delta_o\,(3\,L_V + c_p\,\theta_p)\,]\,. \tag{12}$$

Simple calculations show that the time constant $(1/\zeta)$ is of the order 30 to 60 minutes.

In order to calculate the effect of slab thickness, we must go beyond the surface-pyrolysis calculation inherent in Eq. (3). We assume that pyrolysis takes place in depth, and that the rate is given by an Arrhenius dependence:

$$\dot{m}'''(x) = k_o\,\left[\, e^{-T_A/T(x)} - e^{-T_A/T_o}\,\right] \tag{13}$$

As indicated, the spatial dependence of $\dot{m}'''$ is a consequence of the temperature being a function of depth. Then the production rate from the surface to the depth L is

$$\dot{m}''(L) = \int_0^L \dot{m}'''(x)\, dx \tag{14}$$

Equations (7), (13), and (14) then result in

$$\dot{m}''(L) = k_o\delta\,\left\{E_1(T_A/T_p) - E_1(T_A\,u(L)) + e^{-T_A/T_o}\left[\mathcal{E}i\left(\frac{T_A\,\theta_p}{T_o\,T_p}\right) - \mathcal{E}i\left(\frac{T_A}{T_o}(1-T_o u(L))\right) - \frac{L}{\delta}\right]\right\} \tag{15}$$

where $$u(L) \equiv \left(T_o + \theta_p\, e^{-L/\delta}\right)^{-1}, \tag{16}$$

$$\mathcal{E}i(x) = \int_{-\infty}^{x} \frac{e^t}{t}\, dt \tag{16a}$$

and E_1 is the first exponential integral.

For the semi-infinite slab, $L \to \infty$, and Eq. (15) yields

$$\lim_{L\to\infty} \dot{m}''(L) = k_o\delta\,\left\{E_1(T_A/T_p) - E_1(T_A/T_o) + e^{-T_A/T_o}\left[\mathcal{E}i\left(\frac{T_A\,\theta_p}{T_oT_p}\right) - \gamma - ln\left(\frac{T_A\,\theta_p}{T_o^2}\right)\right]\right\} \tag{17}$$

where γ is Euler's constant.

The activation temperature will be of the order of 20,000 K, so that, with $T_o \approx 300$ K and $T_p \approx 600$ K, $E_1(T_A/T_o) << E_1(T_A/T_p)$ and $\gamma + ln(T_A\theta_p\,/\,T_o^2)$ is much smaller than the other term. Thus

$$\dot{m}''(\infty) \cong k_o\delta\,\left[E_1(T_A/T_p) + e^{-T_A/T_o}\,\mathcal{E}i\left(\frac{T_A\,\theta_p}{T_oT_p}\right)\right]. \tag{18}$$

Indeed, the arguments are sufficiently large that the asymptotic expansion can be used, and we find from Eq. (18) that

$$\dot{m}''(\infty) \cong k_o \delta \frac{T_p^2}{T_A \theta_p} e^{-T_A/T_p} . \quad (19)$$

A similar analysis for the finite-thickness case shows that

$$\frac{\dot{m}''(L)}{\dot{m}''(\infty)} \cong 1 - e^{-pL/\delta} \quad (20)$$

where

$$p \equiv \frac{\theta_p T_A}{T_p^2} . \quad (21)$$

The temperature profile in a thin slab will be different from what it is in a skin of the same thickness, of a thick slab. Nevertheless, we make the simplistic assumption that Eq. (20) holds for a slab of thickness L.

Finally, assuming that any changes in p, L, or δ are slow, this analysis should hold in the more general case; that is,

$$\frac{\dot{m}''(L,t)}{\dot{m}''(\infty,t)} \cong 1 - e^{-p(t)L(t)/\delta(t)} . \quad (22)$$

If the pyrolysis occurs because of heating fluxes from a flame, it is necessary to be able to calculate these. This has been done for a wall fire; it is necessary to point out that the convective flux from the flame is there calculated according to a Spalding-type of expression (Mitler, 1988),

$$\phi_c = \frac{\dot{m}'' B H_V}{exp(\dot{m}'' c_p / h) - 1} . \quad (23)$$

In the present work, the simpler expression

$$\phi_c = h' (T_f - T_s) \quad (24)$$

has been used, where h' is the heat transfer coefficient with blowing, T_f is the mean flame temperature, and T_s is the wall surface temperature.

In order to achieve the same results using either Eq. (23) or (24), with the expression used here for h', it is necessary to take T_f = 1366 K (rather than the 1262 K used in [Mitler, 1988]). However, the earlier data were analyzed assuming that the fires were steady state (Mitler, 1988; Steckler, 1988). In fact, it is apparent that these were *transient* burns which only *appeared* to be steady. In order to obtain these results for the transient condition, it is necessary to take T_f = 1475 K in Eq. (24). This is not realistic, but it probably compensates for a too-low estimate of h'. Other properties used in the present calculation of burning walls of PMMA are given in reference (Mitler, 1988).

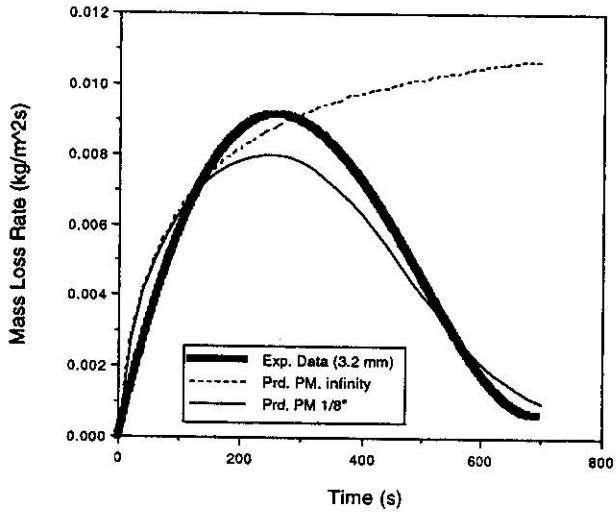

Figure 5. Comparison of measured (thick line) and predicted (thin solid line) values of local mass loss rate for 3.2 mm thick PMMA; also shown is prediction for semi-infinite PMMA Slab.

Analysis of the data of Kashiwagi and Ohlemiller (1982) according to the equations above, yields $T_A \cong$ 14,430 K for PMMA. With that value, an assumed fixed pyrolysis temperature T_p = 630 K, and an assumed mean flame temperature T_f = 1475, calculations give the mass-loss rates as shown in Fig. 5.

Discussion

Figures 3 and 4 show mass loss per unit area and mass loss rate as a function of time for three different wall materials. It can be noted that the mass loss rate is far from being a constant or "steady state" value. This is especially important in case of estimating total energy release rate or for predicting upward flame spread rate on a wall. A vertical wall burns at a different rate at various locations depending on the history of ignition of the location even though the local mass rate is completely insensitive to the actual vertical location *per se*. The cumulative mass rate can then be calculated only by integrating the mass loss rate over the entire height. The cardboard clearly burns in a very different manner compared to the other two materials. It should be noted here that the local mass loss rate function is strongly dependent on the thickness. The local mass rate functions

shown here may be used as "fire properties" in room fire or flame spread models.

Figure 5 shows comparison of data and predictions for a 3.2 mm PMMA slab. The solid curve is for an assumed 3.2 mm-thick sheet of PMMA; the dashed curve is for an infinitely thick slab. The asymptotic value is 11.65 g/m^2s. We note that the calculated peak value occurs at about t = 246 s, and is about 13% below the experimental value. This is an excellent agreement considering that this is only an approximate analysis, involving many assumptions and simplifications. Moreover, there are significant differences among samples of PMMA.

It is also noteworthy that this simple model yields a mass loss rate which is in proportion to the thickness of the sample, so that it goes gradually to zero, whereas the experimental results show burn-through at a well-defined time. In future work, it will be useful to develop an algorithm for materials with more complex behavior, such as charring, dripping, laminated, and composite materials.

Conclusion

The time-dependent local mass loss rate of finite-thickness burning vertical walls made of PMMA is modeled and compared with experimental data. Such data or predictions are needed, for example, in room fire hazard analysis models to estimate total energy release rate or upward flame spread rate.

The experimental setup adequately simulates a burning wall with turbulent flames in a typical room fire situation because the magnitude of flame heat feedback is close to that of flames occurring in a room fire (having a scale of around 2 m). Thus the data obtained in this apparatus may be used as a "fire property" of the wall material for modeling purposes. Even though the data and predictions are compared only for 3.2 mm thick PMMA slabs, experiments can be easily extended to describe time dependent behavior of the local mass loss rate for practical vertical wall materials with such complexities as charring, dripping, and composite structure.

Predictions made by the proposed model compare remarkably well considering the lack of accurate property data available and simplicity of the model. It will be useful to extend the model to include behavior of practical materials such as woods, plastics, and laminated materials.

References

Ahmad, T. and Faeth, G. M., Journal of Heat Transfer 100, p. 112 (1978).

Delichatsios, M. and de Ris, J., An Analytical Model of the Pyrolysis for Charring Materials , Technical Report no. 0K0J1.BU, Factory Mutual Research Corp., Norwood, MA (May, 1983).

Delichatsios, M.A., Twenty-First Symposium (Int'l) on Combustion , the Combustion Institute, Pittsburgh, PA., p. 53 (1987).

Kashiwagi, T. and Ohlemiller, T.J., 19th Symposium (Int'l) on Combustion , the Combustion Institute, Pittsburgh, PA., p. 815 (1982).

Kim, C.I. and Kulkarni, A.K., Combustion Science and Technology vol.73, p. 493-504 (1990a).

C. I. Kim and A. K. Kulkarni, The Eastern Section of the Combustion Institute, 1990 Fall Technical Meeting, Orlando, Florida, p. 52, December 3-5 (1990b).

Kim, J., de Ris, J., and Kroesser, F.W., Thirteenth Symposium (Int'l) on Combustion , The Combustion Institute, Pittsburgh, PA, p. 949 (1971).

Kosdon, F., Williams, F.A., and Buman, C., Twelfth Symposium (Int'l) on Combustion , The Combustion Institute, Pittsburgh, PA, p. 252 (1969).

Mitler, H.E., Fire Safety Science, Proceedings of the Second International Symposium (Eds., C.E. Grant and P.J. Pagni), Hemisphere Publishing Co. (1988).

Orloff, L., Modak, A.T., and Alpert, R.L., Sixteenth Symposium (Int'l) on Combustion , The Combustion Institute, Pittsburgh, PA. p. 1345 (1977).

Quintiere, J. G., Harkleroad, M. and Hasemi, Y., Combustion Science and Technology 48, p. 191 (1986).

Quintiere, J.G., Journal of Research of the National Bureau of Standards 93, p. 61 (1988).

Steckler, K.D. and Mitler, H.E., Proceedings of the Fall Technical Meeting, The Eastern Section of The Combustion Institute, Clearwater Beach, Florida, p. 73-1(December 1988).

The experimental portion of the work was conducted at The Pennsylvania State University and it was supported under grant no. 60NANB8D0849 by the Building and Fire Research Laboratory, National Institute of Standards and Technology, Gaithersburg, MD. The theoretical portion of the work was conducted at the National Institute of Standards and Technology, Gaithersburg, MD.